

Supporting Information

for

Isotropic and Anisotropic Growth of Metal-Organic Framework (MOF) on MOF: Logical Inference on MOF Structure Based on Growth Behavior and Morphological Feature

Sora Choi, Taeho Kim, Hoyeon Ji, Hee Jung Lee, and Moonhyun Oh*

Department of Chemistry, Yonsei University, 50 Yonsei-ro, Seodaemun-gu, Seoul 120-749,
Korea

Fax: (82) 2-364-7050.

Phone: (82) 2-2123-5637

Email: moh@yonsei.ac.kr

General Methods

Solvents and all other chemicals were obtained from commercial sources and used as-received unless otherwise noted. All scanning electron microscopy (SEM) images were obtained using a JEOL JSM-6701F field-emission SEM. All transmission electron microscopy (TEM) and scanning transmission electron microscopy (STEM) images were acquired on a FEI Tecnai G2 F30 ST instrument at 300 kV. Energy dispersive X-ray (EDX) spectra, EDX spectrum profile scanning data, and elemental mapping images were obtained using an STEM attachment (Korea Basic Science Institute, Seoul, Korea). The selected area electron diffraction (SAED) patterns were acquired with a JEOL JEM-2100F at 200 kV (Center for Microcrystal Assembly, Sogang University). The simulated SAED patterns were acquired using the software SingleCrystal Ver. 2.3.3. X-ray diffraction patterns were obtained using a Rigaku Ultima IV instrument equipped with a graphite-monochromated CuK α radiation source (40 kV, 40 mA). The sorption isotherms of N₂ (77 K) were measured in the gaseous state using a BELSORP Max volumetric adsorption equipment. All gas adsorption isotherms were measured after pretreatment under a dynamic vacuum at 250 °C for 12 h. ¹H NMR spectra were recorded on a Bruker Advance II 400 spectrometer (¹H NMR, 400 MHz) with chemical shifts reported relative to residual deuterated solvent peaks. MDI Jade 9.0 software (Materials Data Inc., Livermore, CA) was used to calculate the cell parameters of product. Thermogravimetric analysis (TGA) measurements were performed using a Shimadzu TGA-50 in a nitrogen atmosphere. The infrared (IR) spectra of solid samples were obtained using a Jasco FT-IR 4200 LE spectrometer.

Preparation of CPP-I of MIL-68.¹ A precursor solution was prepared by mixing 1,4-benzenedicarboxylic acid (3.0 mg, 0.018 mmol) and In(NO₃)₃·xH₂O (7.8 mg, 0.020 mmol) in 0.8

mL of *N,N*-dimethylformamide (DMF). The resulting mixture was placed in an oil bath (100 °C) for 10 min. The hexagonal rods generated after this time were isolated by cooling the reaction mixture to room temperature, collecting the precipitate by centrifugation, and washing several times with fresh DMF and methanol. Each successive supernatant was decanted and replaced with fresh solvents. ATR-FTIR (cm^{-1}): 1563s, 1506m, 1432m, 1393s, 1316w, 1290w, 1252w, 1158w, 1103w, 1020w, 876m, 823w, 813w, 746m.

Preparation of CPP-II of MIL-68-Br. A precursor solution was prepared by mixing 2-bromoterephthalic acid (4.4 mg, 0.018 mmol) and $\text{In}(\text{NO}_3)_3 \cdot x\text{H}_2\text{O}$ (7.8 mg, 0.020 mmol) in 0.8 mL of DMF. The resulting mixture was placed in an oil bath (100 °C) for 20 min. Thin hexagonal rods were isolated by cooling the reaction mixture to room temperature, collecting the precipitate by centrifugation, and washing several times with fresh DMF and methanol. Each successive supernatant was decanted and replaced with fresh solvents. ATR-FTIR (cm^{-1}): 1573s, 1482w, 1395s, 1281w, 1255w, 1154w, 1041w, 903m, 889m, 827w, 806w, 767m, 728w, 661w.

Preparation of CPP-III of MOF-NDC. A precursor solution was prepared by mixing naphthalene-1,4-dicarboxylic acid (3.9 mg, 0.018 mmol) and $\text{In}(\text{NO}_3)_3 \cdot x\text{H}_2\text{O}$ (7.8 mg, 0.020 mmol) in 0.8 mL of DMF. The resulting mixture was placed in an oil bath (100 °C) for 20 min. The square rods were isolated by cooling the reaction mixture to room temperature, collecting the precipitate by centrifugation, and washing several times with fresh DMF and methanol. Each successive supernatant was decanted and replaced with fresh solvents. ATR-FTIR (cm^{-1}): 1579m, 1549s, 1519m, 1461m, 1415s, 1368s, 1317w, 1267w, 1211w, 1169w, 1040w, 984w, 960w, 881m, 823w, 785m, 745w, 666w, 629w.

Preparation of MIL-68 template.¹ Pyridine (0.036 mmol) was added to the precursor solution of 1,4-benzenedicarboxylic acid (3.0 mg, 0.018 mmol) and In(NO₃)₃·xH₂O (7.8 mg, 0.020 mmol) dissolved in 0.9 mL of *N,N*-dimethylformamide (DMF) was added to 2 equiv. of pyridine. The resulting mixture was placed in an oil bath (100 °C) for 10 min. The hexagonal lumps generated after this time were isolated by cooling the reaction mixture to room temperature, collecting the precipitate by centrifugation, and washing several times with fresh DMF and methanol. Each successive supernatant was decanted and replaced with fresh solvents.

Preparation of hybrid-CPP-II of MIL-68@MIL-68-Br. A precursor solution was prepared by mixing 2-bromoterephthalic acid (4.4 mg, 0.018 mmol) and In(NO₃)₃·xH₂O (7.8 mg, 0.020 mmol) in 0.8 mL of DMF. An MIL-68 template (2.0 mg) was then introduced to the precursor solution. The resulting mixture was placed in an oil bath (100 °C) for 20 min. The long hexagonal rods generated after this time were isolated and subsequently washed with fresh DMF and methanol via centrifugation-redispersion cycles. ATR-FTIR (cm⁻¹): 1566s, 1506w, 1482w, 1431w, 1392s, 1316w, 1284w, 1253w, 1157w, 1103w, 1042w, 1020w, 906w, 879m, 825w, 813w, 767w, 746m, 728w, 660w.

Preparation of hybrid-CPP-III of MIL-68@MOF-NDC. A precursor solution was prepared by mixing naphthalene-1,4-dicarboxylic acid (3.9 mg, 0.018 mmol) and In(NO₃)₃·xH₂O (7.8 mg, 0.020 mmol) in 0.8 mL of DMF. An MIL-68 template (2.0 mg) was then introduced to the precursor solution. The resulting mixture was placed in an oil bath (100 °C) for 20 min. The semi-tubular-type hexagonal rods generated after this time were isolated and subsequently washed with fresh DMF and methanol via centrifugation-redispersion cycles. ATR-FTIR (cm⁻¹):

1564s, 1551s, 1506w, 1462w, 1416m, 1393s, 1370m, 1316w, 1290w, 1269w, 1212w, 1169w,
1159w, 1103w, 1020w, 879m, 824w, 813w, 787w, 775w, 746m, 667w, 630w.

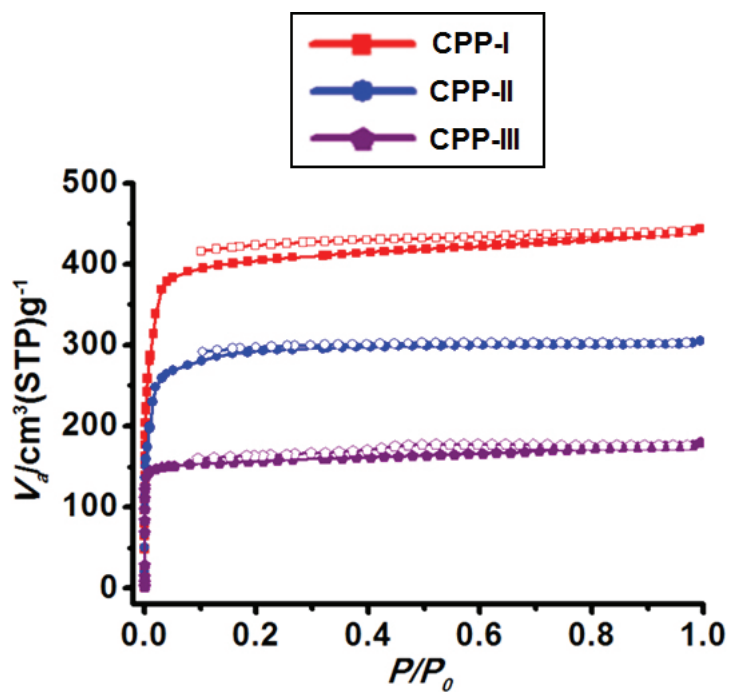


Figure S1. N₂ sorption isotherms of CPP-I–CPP-III (CPP-I; red, CPP-II; blue, CPP-III; purple). N₂ sorption isotherms of CPP-I–CPP-III displayed type I behavior, typical of microporous materials. See Supplementary Table S1 for the surface areas and total pore volumes of CPP-I–CPP-III.

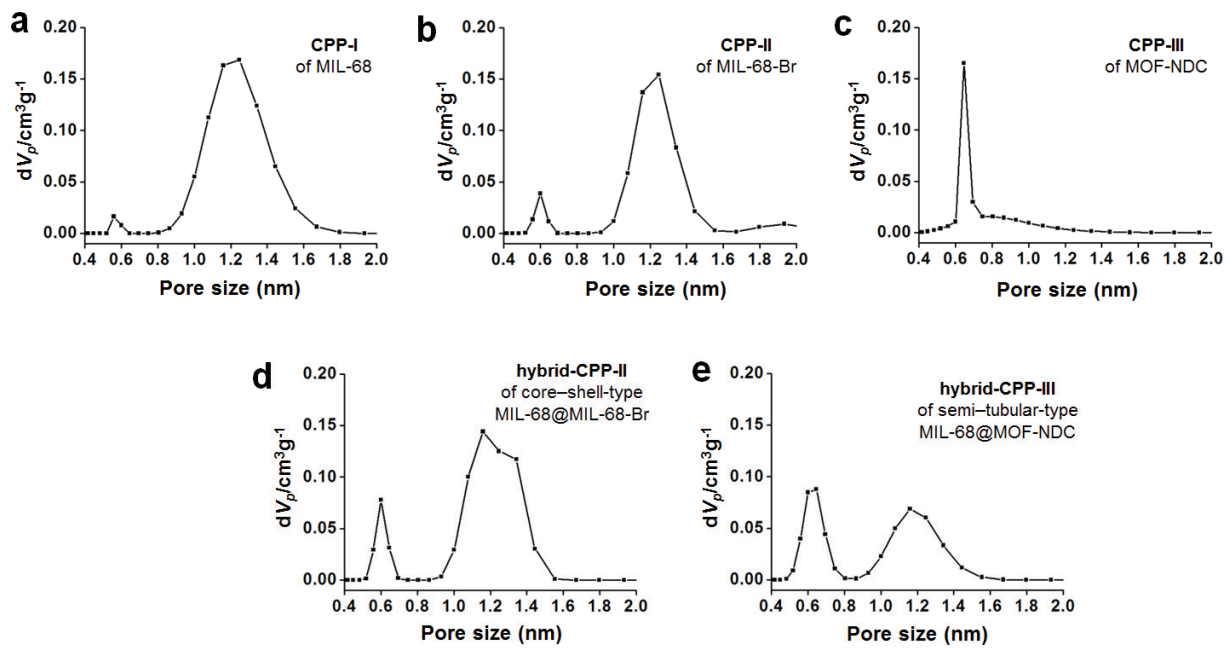


Figure S2. Pore size distributions calculated from the non-local density functional theory (NLDFT) method. (a) **CPP-I** of MIL-68, (b) **CPP-II** of MIL-68-Br, (c) **CPP-III** of MOF-NDC, (d) **hybrid-CPP-II** of MIL-68@MIL-68-Br, and (e) **hybrid-CPP-III** of MIL-68@MOF-NDC.

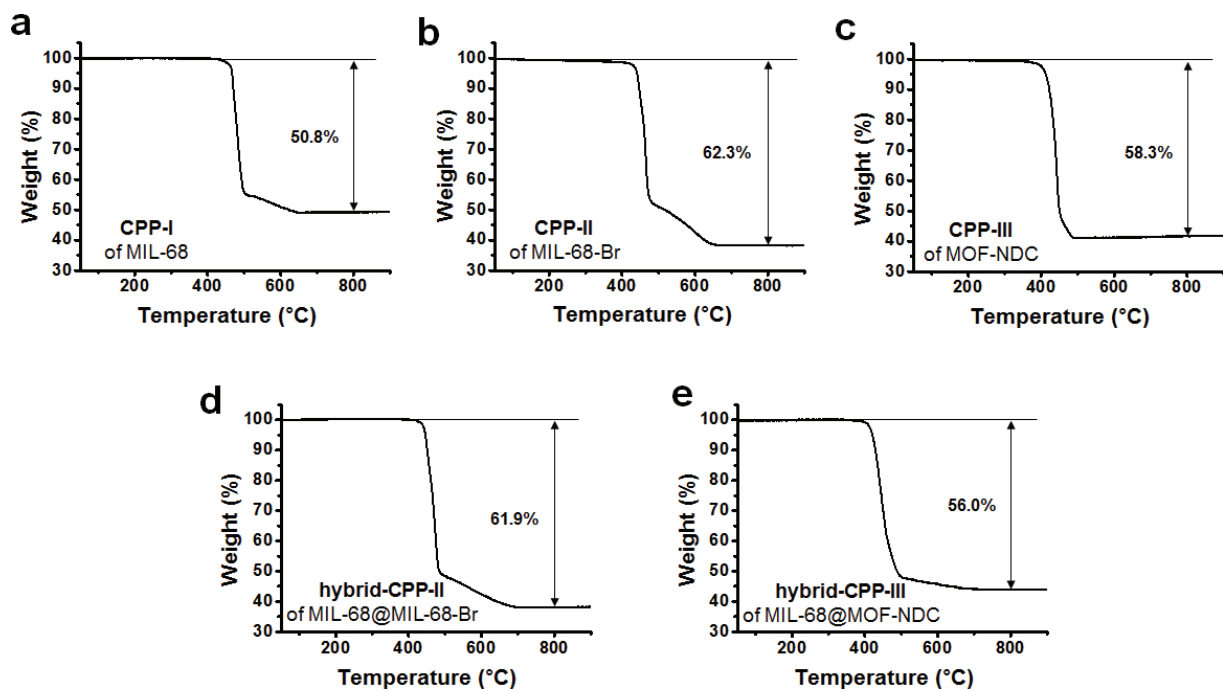


Figure S3. TGA curves of (a) **CPP-I** of MIL-68, (b) **CPP-II** of MIL-68-Br, (c) **CPP-III** of MOF-NDC, (d) **hybrid-CPP-II** of MIL-68@MIL-68-Br, and (e) **hybrid-CPP-III** of MIL-68@MOF-NDC.

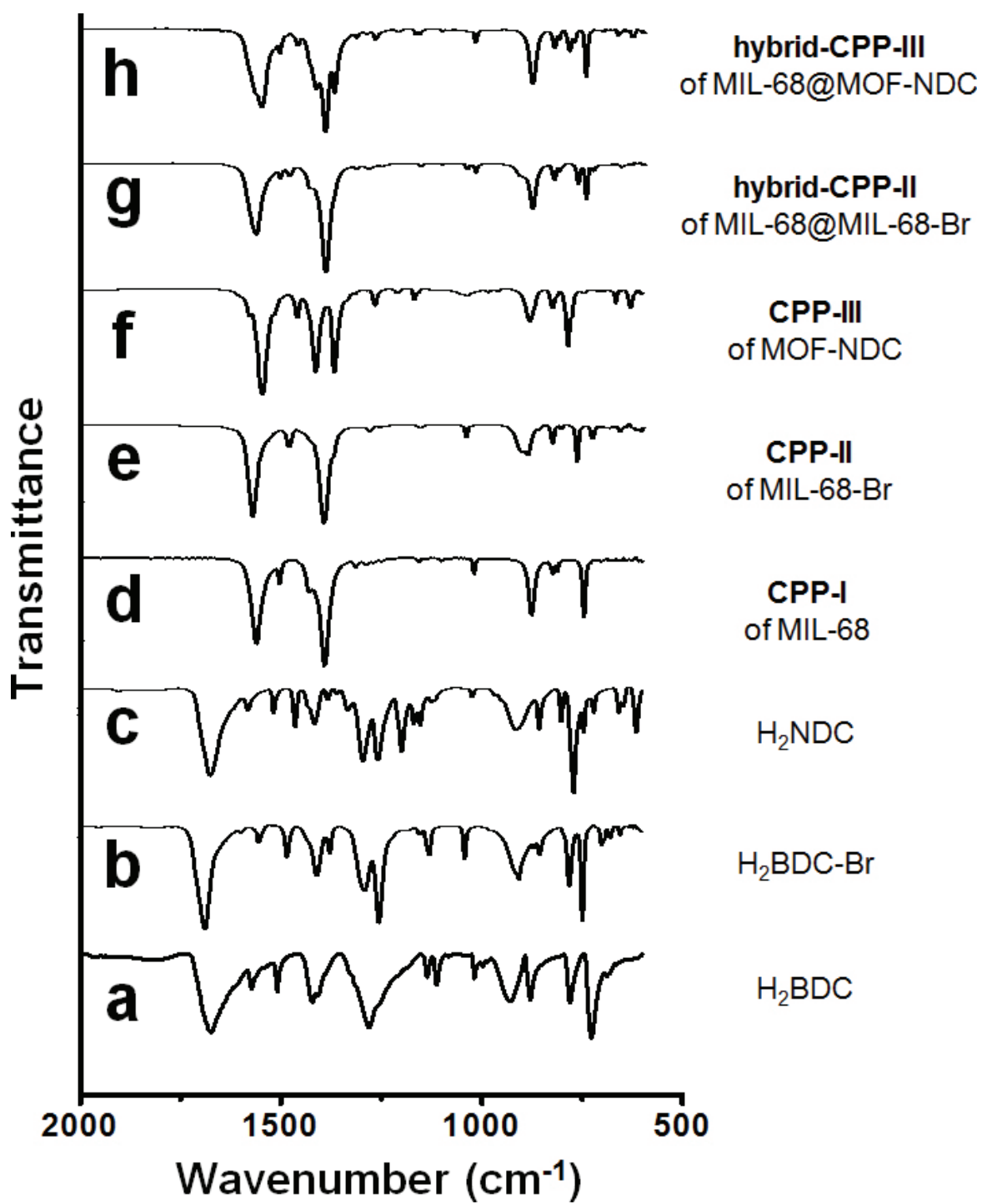


Figure S4. IR spectra of (a) H₂BDC, (b) H₂BDC-Br, (c) H₂NDC, (d) **CPP-I** of MIL-68, (e) CPP-II of MIL-68-Br, (f) CPP-III of MOF-NDC, (g) **hybrid-CPP-II** of MIL-68@MIL-68-Br, and (h) **hybrid-CPP-III** of MIL-68@MOF-NDC.

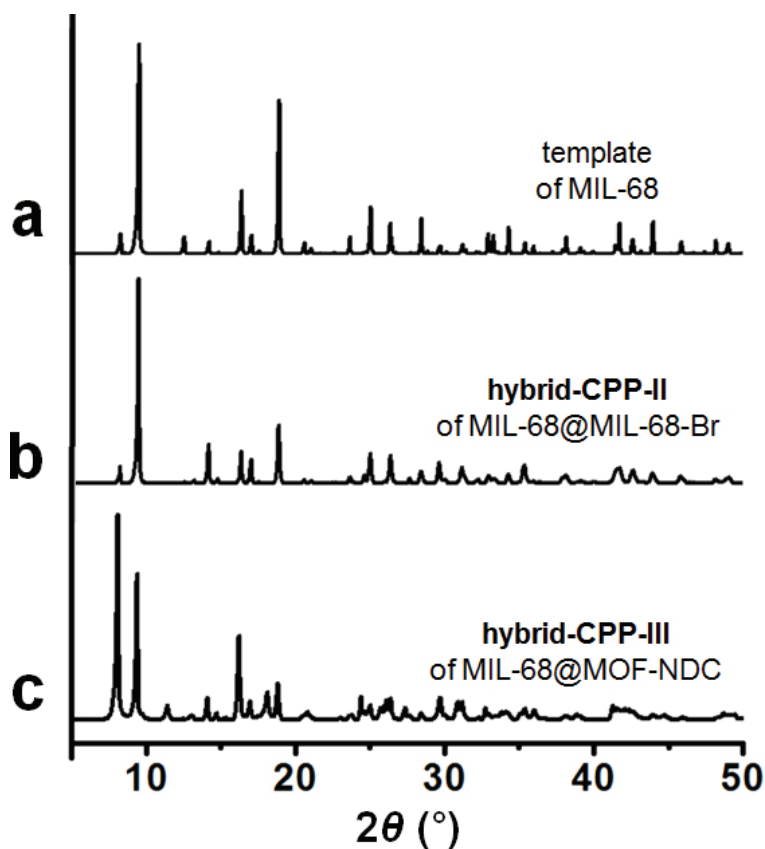


Figure S5. PXRD patterns of (a) the initial micro-template of MIL-68, (b) **hybrid-CPP-II** of MIL-68@MIL-68-Br constructed from the isotropic growth of MIL-68-Br on the MIL-68 template, and (c) **hybrid-CPP-III** of MIL-68@MOF-NDC constructed from the anisotropic growth of MOF-NDC on the MIL-68 template. Two different structures (MIL-68 and MOF-NDC structures) are present within **hybrid-CPP-III**.

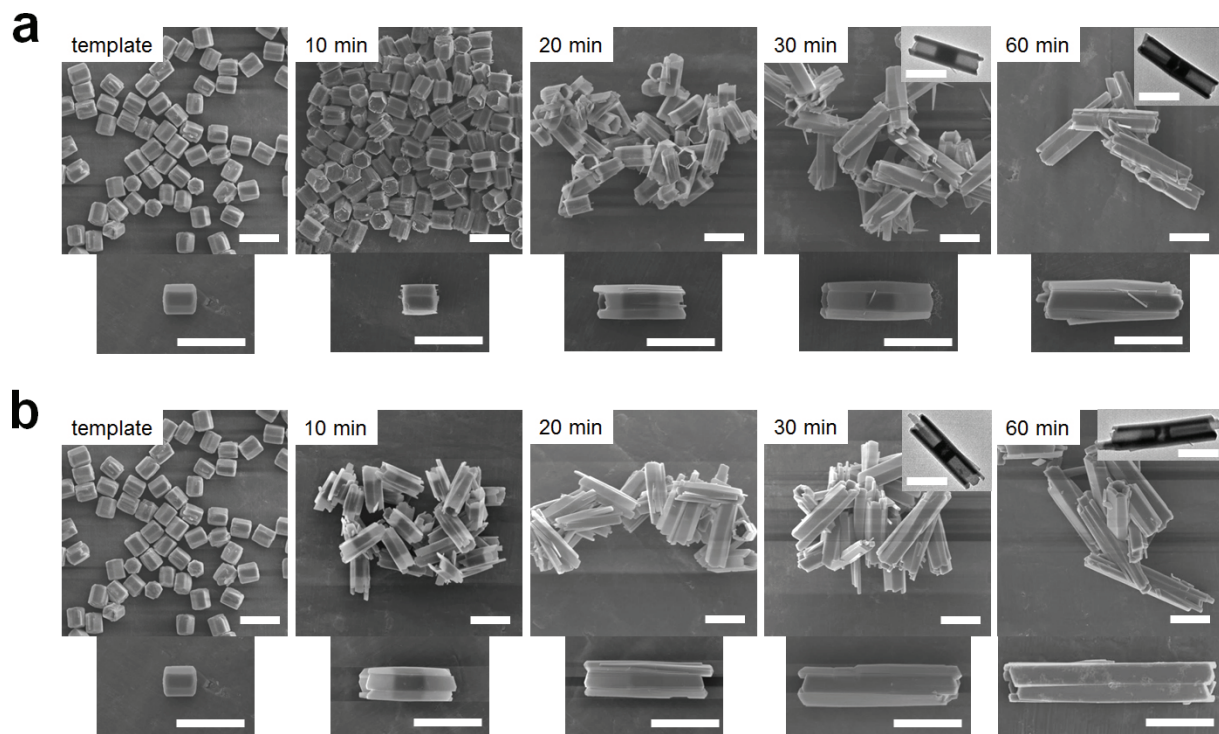


Figure S6. (a) SEM and TEM images of **hybrid-CPP-III** obtained by increasing the reaction time (~ 60 min) in the presence of H₂NDC (3.9 mg), In(NO₃)₃ (7.8 mg), and MIL-68 template (2.0 mg). (b) SEM and TEM images of **hybrid-CPP-III** obtained in the presence of excess amounts of H₂NDC (7.8 mg) and In(NO₃)₃ (15.6 mg) with keeping the same amount of MIL-68 template (2.0 mg) at various times. Scale bars are 5 μ m.

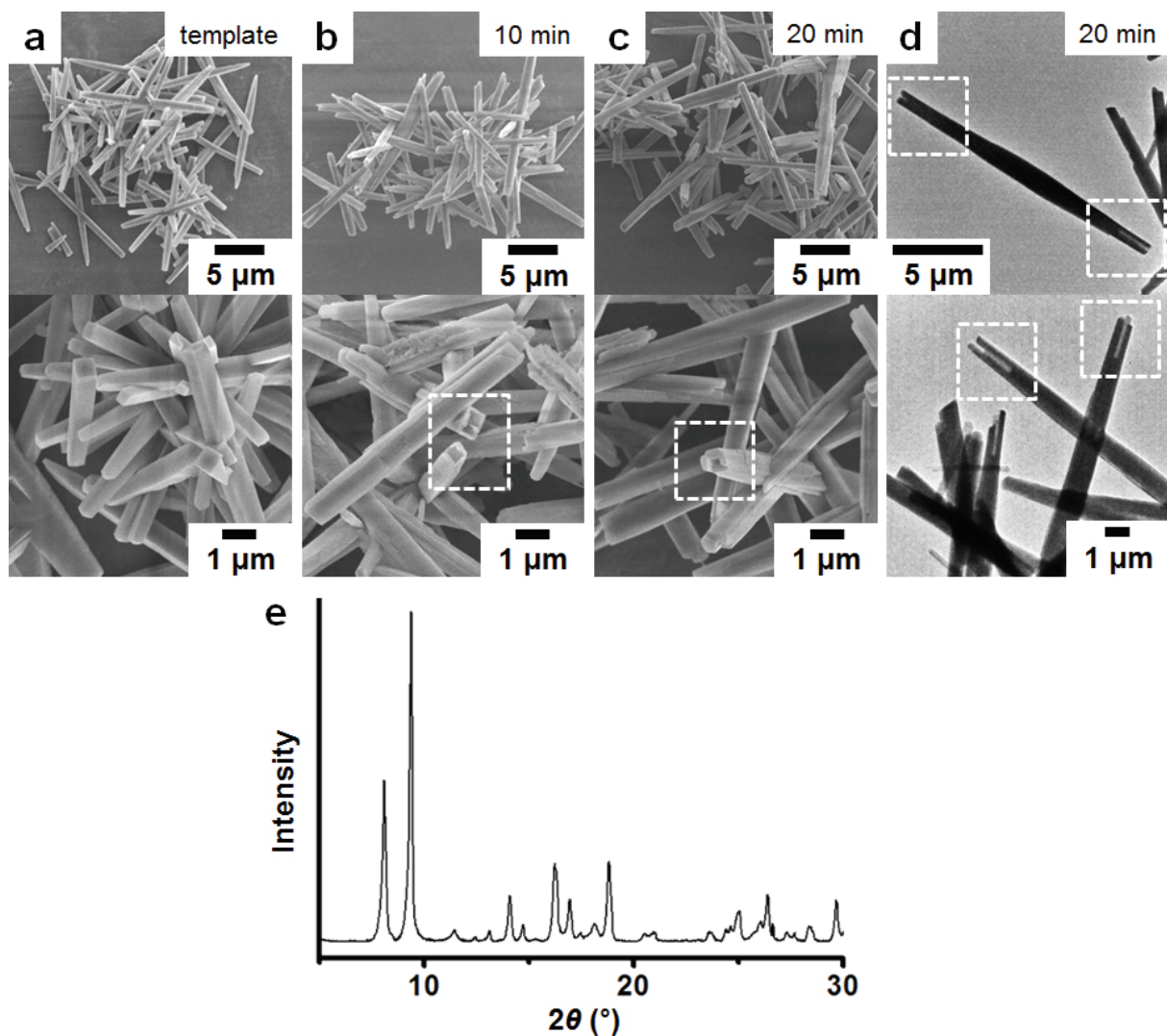


Figure S7. (a) SEM images of the initial templates of MOF-NDC. (b) SEM images of the products obtained from the growth of MIL-68 on the MOF-NDC template during 10 min. (c) SEM images, (d) TEM images, and (e) PXRD pattern of the products obtained from the growth of MIL-68 on the MOF-NDC template during 20 min. Products in the boxes show the semi-tubular shape. The PXRD pattern shows the co-existence of both MIL-68 and MOF-NDC structures within the particles. All peaks from both MIL-68 core and MOF-NDC shell were found in the PXRD pattern.

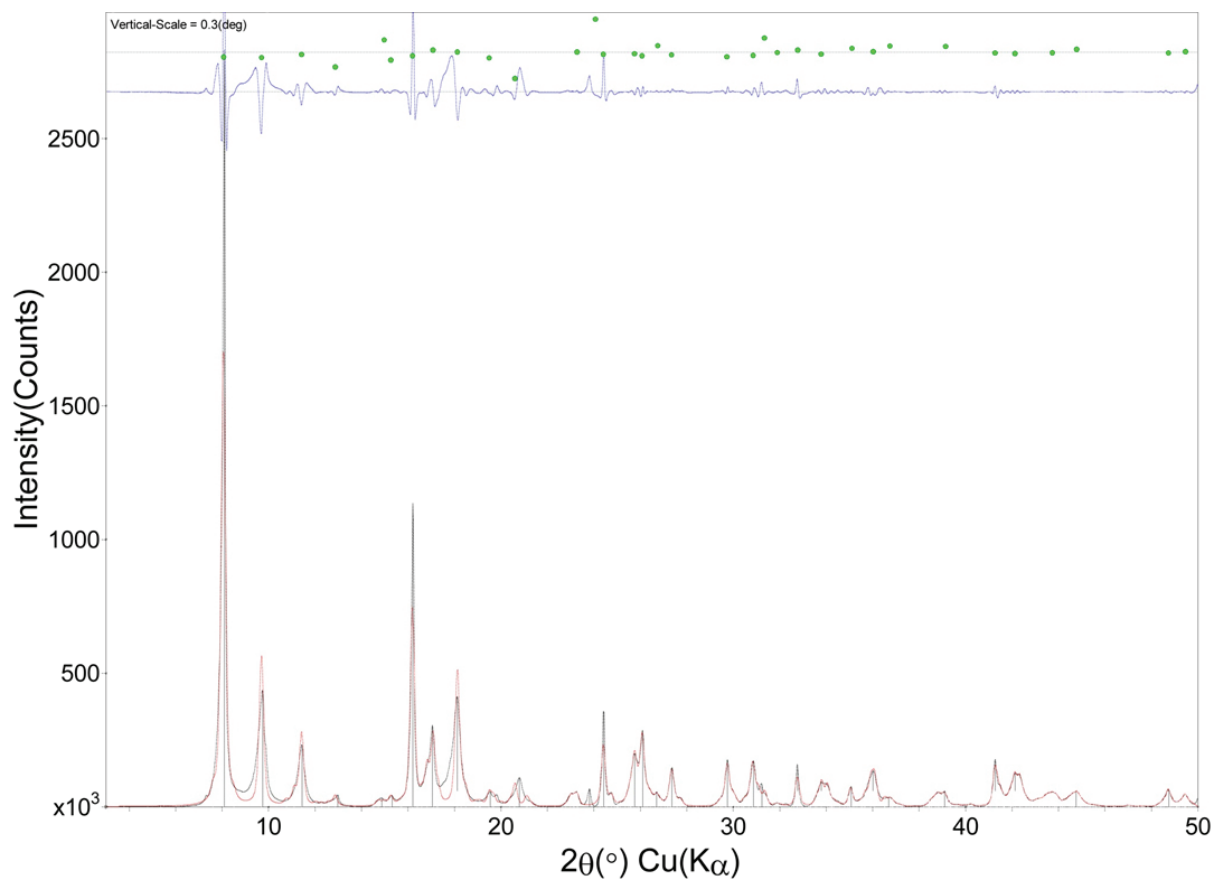


Figure S8. Whole pattern fitting of **CPP-III** (MOF-NDC). The black line is the experimental PXRD pattern and the red line is the calculated PXRD pattern. The top blue line indicates the deviation between the experimental and calculated PXRD patterns. The unit cell parameters of MOF-NDC calculated using MDI Jade 9.0 software were $a = b = 32.765 \text{ \AA}$, $c = 7.182 \text{ \AA}$, and $\alpha = \beta = \gamma = 90^\circ$.

Table S1. Surface areas and total pore volumes of **CPP-I–CPP-III**, **hybrid-CPP-II**, and **hybrid-CPP-III**.

CPP	Surface area [m ² g ⁻¹]	Total pore volume [cm ³ g ⁻¹]
CPP-I	1564	0.69
CPP-II	1062	0.47
CPP-III	597	0.27
hybrid-CPP-II	1346	0.58
hybrid-CPP-III	1021	0.46

Table S2. Relative amounts of core and shell portions within **hybrid-CPP-II** and **hybrid-CPP-III**.

Hybrid CPP	Core		Shell	
	Material	Relative amount ^[1]	Material	Relative amount ^[1]
hybrid-CPP-II	MIL-68	1	MIL-68-Br	3.65
hybrid-CPP-III	MIL-68	1	MOF-NDC	1.11

[1] These values were obtained from ¹H NMR spectrum analysis (integration of the peaks correlated to H₂BDC, and H₂BDC-Br or H₂NDC) of hybrid CPPs digested in a co-solvent of acetic acid-d⁴ and DMSO-d⁶.

Reference

- (1) Cho, W.; Lee, H. J.; Oh, M. *J. Am. Chem. Soc.* **2008**, *130*, 16943-16946.